Ionic Liquid–Induced Changes in Properties of Aqueous Cetyltrimethylammonium Bromide: A Comparative Study of Two Protic Ionic Liquids with Different Anions

ARTICLE *in* THE JOURNAL OF PHYSICAL CHEMISTRY B · MARCH 2011

Impact Factor: 3.3 · DOI: 10.1021/jp200233q · Source: PubMed

7 AUTHORS, INCLUDING:

Vishal Govind Rao
Bowling Green State University
49 PUBLICATIONS **533** CITATIONS
SEE PROFILE

Chiranjib Ghatak
University of Kansas
38 PUBLICATIONS **570** CITATIONS
SEE PROFILE

Sarthak Mandal
Columbia University
44 PUBLICATIONS **444** CITATIONS
SEE PROFILE

Nilmoni Sarkar
IIT Kharagpur
159 PUBLICATIONS **3,689** CITATIONS
SEE PROFILE

THE JOURNAL OF PHYSICAL CHEMISTRY B

ARTICLE

pubs.acs.org/JPCB

Ionic Liquid-Induced Changes in Properties of Aqueous Cetyltrimethylammonium Bromide: A Comparative Study of Two Protic Ionic Liquids with Different Anions

Vishal Govind Rao, Chiranjib Ghatak, Surajit Ghosh, Rajib Pramanik, Souravi Sarkar, Sarthak Mandal, and Nilmoni Sarkar*

Department of Chemistry, Indian Institute of Technology, Kharagpur 721302, WB, India

ABSTRACT: In this work we have shown a comparative study of changes in physicochemical properties of an aqueous solution of a common cationic surfactant cetyltrimethylammonium bromide (CTAB) upon addition of two protic ionic liquids dimethylethanol ammonium hexanoate (DAH) and dimethylethanol ammonium formate (DAF). The aim of this manuscript is to offer a comparative study and establish the role of the alkyl chain length of the anion of the added protic ionic liquids on the physicochemical properties of aqueous solution of CTAB. At lower concentration (i.e., ≤ 30 mM) both ionic liquids show the same trend in modifying the properties of aqueous CTAB solution, but DAH as an additive shows a more dramatic increase in aggregation number and size of the CTAB micelle compared to that of DAF as an additive. At higher concentrations of additives (DAF and DAH), the properties of aqueous CTAB solution change in an entirely different way. The size of the CTAB micelle was found to be 0.9 nm. With the addition of 215 mM DAH, the size of the CTAB micelle increases to 25.0 nm, whereas with the addition of 215 mM DAF it increases to only 5.6 nm. Zeta potential, electrical conductance, microviscosity, and dipolarity measurements were performed to gain insight into this abrupt size change in the case of DAH. It is proposed that the formate and hexanoate anions undergo Coulombic attractive interaction with cationic head groups of the CTAB micelle at all concentrations. In the case of DAH, the presence of a hexyl chain on the hexanoate ion allows it to align with the tail part of CTAB, whereas in the case of DAF the absence of an alkyl chain in the formate ion is apparently unable to align the formate anion with the tail part of CTAB. So this difference in the location of the anions of DAF and DAH is responsible for the different size changes and different behaviors of the two ionic liquids.

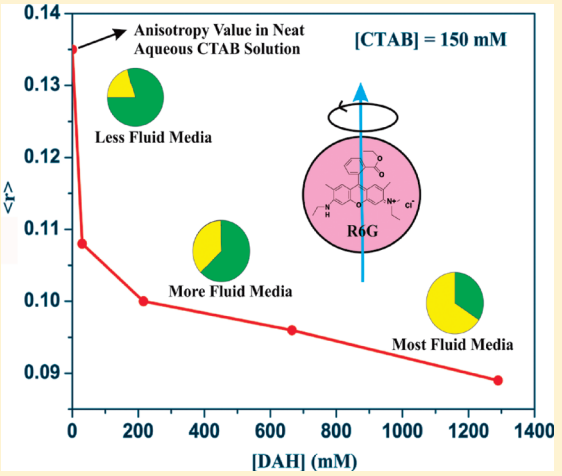

1. INTRODUCTION

Due to widespread application of surfactant-based systems, the self-assembly of surfactant molecules into a large variety of nano-, micro-, and macrostructures is of fundamental interest and plays a significant role in many important applications such as nanomaterial synthesis,[1−3] drug delivery,[4,5] separations,[6] pharmaceutical formulations, and other dispersant technologies.[6,7] Probing the interfacial and thermodynamic properties of surfactants in solution, both in the presence and in the absence of additives, can provide extensive information about solute−solute and solute−solvent interactions of the surfactant in solution. The interfacial and micellar properties of surfactant solutions are governed by a finespun balance of solvophobic and solvophilic interactions. These characteristics can be modified in two ways: (i) through specific interactions with the surfactant molecules (solubilization of cosolvent to the micelle) and (ii) by changing the nature of the solvent. The solvent quality can be altered by adding different amounts of a cosolvent to the aqueous solution, with this providing the opportunity to study the influence of cosolvent addition on the hydrophobic effect on micellization.[8] Such studies on the effects of cosolvents on the aggregation and other physicochemical properties of surfactants are of fundamental and industrial interest.[9] To date there has been limited number of solvents that are generally recognized as self-assembly media.[10,11] One can increase the number of these solvents by understanding and manipulating the molecular interactions involved in amphiphile self-assembly. Self-assembly of surfactants in contact with ionic liquids (ILs) thereby forming micelles,[12−14] microemulsions,[15−17] liquid crystals,[18] gels,[19] and vesicles[20] has been extensively explored.

There are many reports focusing on the change in behavior of aqueous surfactant solutions with the addition of different alcohols. Two theories have been proposed to explain the effect of alcohols on micelles: the first one deals primarily with the solubilization of alcohols in micelles, and the other one deals with the effects of the alcohols on the solvent structure. The first put forth by Emerson and

Received: January 9, 2011
Revised: February 14, 2011
Published: March 18, 2011

Holtzer[21] and others[22,23] classified the organic additives into two categories: penetrating and nonpenetrating. Nonpenetrating additives putatively affect micelle stability by altering the dielectric constant of water and by providing hydrophobic contacts for hydrocarbon chains at the micellar surface. Penetrating additives increase the stability of the micelle by decreasing the surface charge density through incorporation of the hydrocarbon portion of the additive between the soap chains just below the micelle surface. The second theory proposes that additives have a direct effect on the water structure:[24−26] structure makers stabilizes the micelle, while structure breakers have the opposite effect.[24] Nowadays modifying physicochemical properties of aqueous surfactant solutions in favorable fashion by the addition of environmentally benign room-temperature IL (RTIL) has received enormous attention. Due to its unusual properties, an IL may demonstrate a unique role in altering the properties of aqueous surfactant solutions.

Pandey et al. have shown the change in the behavior of aqueous surfactant solutions with the addition of RTILs.[27] One can attempt to understand the effect of ILs on the micellar and biological system considering ILs as salt solutions (salt effect, the so-called Hofmeister effect[28]). In a micellar system, salt addition reduces the repulsions between the head groups of the surfactants; this increases the stability of the micelle and leads to the lowering of the critical micellar concentration (CMC). However, the effect of IL addition is not so simple to understand. The effect of RTILs on CMC is nonmonotonic. The CMC of sodium dodecyl sulfate (SDS), decreases with addition of RTILs in low concentration, but increases with addition of RTILs in high concentration.[27a] In many cases, addition of the IL does not alter the CMC value to a great extent, but the structure is modified to a great extent.[27b]Zheng et al. showed that addition of the IL 1-butyl-3-methylimidazolium bromide ([bmim][Br]) affects aggregation of the triblock copolymer Pluronic P104, and at a high concentration of the RTIL (>1 M) very large aggregates with a diameter of ∼500 nm are formed.[29] Recently, Dey et al. showed that the addition of IL (RTIL, [pmim][Br]) to a 5 wt % triblock copolymer (P123) micelle leads to the formation of giant P123-RTIL clusters of 40 nm in 0.9 M and 3500 nm in 3 M RTIL.[30] They are much larger than the P123 micelle (18 nm).

In this manuscript, we have shown a comparative study of changes in the physicochemical properties of an aqueous solution of a common cationic surfactant cetyltrimethylammonium bromide (CTAB) upon addition of two protic ionic liquids (PILs) dimethylethanol ammonium hexanoate (DAH) and dimethylethanol ammonium formate (DAF). PILs are subset of ionic liquids (ILs), which are easily produced through the combination of a Brønsted acid and Brønsted base. PILs have not received a particularly large share of the literature on ILs.[31] This is despite their having many useful properties and potential applications,[31] often arising from their protic nature, including as self-assembly media,[18,32−35] as reaction media and catalysts for organic reactions,[36−38] in biological applications,[39−42] as proton conducting electrolytes for polymer membrane fuel cells,[43−45] and as explosives.[46−48] The key properties that distinguish PILs from other ILs is the proton transfer from the acid to the base, leading to the presence of proton-donor and -acceptor sites, which can be used to build up a hydrogen-bonded network. It is noteworthy that the two PILs, which we have used, bear the same cationic part, whereas the anionic part differs in the alkyl chain length only. Due to its large alkyl chain length, DAH is more hydrophobic compared to DAF, and it is expected that the two ILs modify the physicochemical properties such as the CMC and aggregation number in different ways. The aim of this paper is to offer a comparative study and establish the role of the alkyl chain length of the anion of the added IL on the physicochemical properties of an aqueous solution of CTAB. Finally, with the future goal of building up (i) proton exchange fuel cells where PILs can act as proton mediators[49,50] and (ii) mixed micelles where the PILs can act as cosurfactants for micellar catalysis, we want to ascertain the effects that these compounds produce on commonly studied and characterized surfactants such as CTAB in aqueous solution.

Scheme 1. Structures of ILs DAF and DAH, Fluorescence Probes pyrene and R6G, Quencher CPC, and Cationic Surfactant CTAB

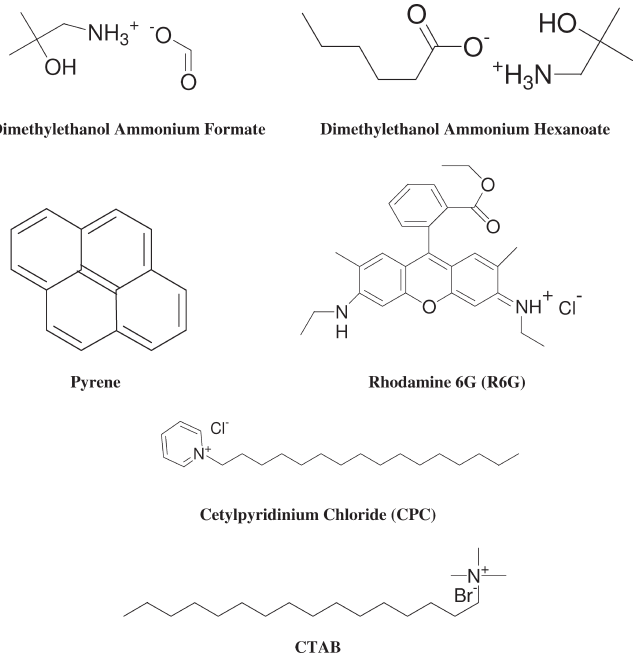

2. EXPERIMENTAL SECTION

2.1. Materials and Sample Preparation. CTAB, pyrene, and cetylpyridinium chloride (CPC), were purchased from Sigma-Aldrich and used as received. Rhodamine 6G (R6G) (laser grade, Exciton) was used as received. DAF and DAH were obtained from Bioniqs (>99% purity) and were also used as received. Doubly distilled deionized water (Milli-Q water) was used for sample preparation. The stock solutions of pyrene and CPC were prepared in ethanol and water, respectively. The final concentration of probe molecule (pyrene) in all the measurements was kept at 5×10^{-7} M. Aqueous CTAB solutions of the probe were prepared taking appropriate aliquots of the probe from the stock and evaporating ethanol using stream of nitrogen gas. Aqueous CTAB of desired concentration was added to achieve the required final probe concentration. The calculated amounts of PILs were added directly to the aqueous CTAB solutions. All the experiments were performed at 298 K. The structures of DAF, DAH, pyrene, R6G, CPC, and cationic surfactant CTAB are shown in Scheme 1.

2.2. Instrumentation. The fluorescence spectra were recorded using a Hitachi (model no. F-7000) spectrofluorimeter. All the samples were excited at 337 nm. For size, ζ potential, and conductivity measurements, we used a Malvern Nano ZS instrument employing a 4 mW He−Ne laser operating at a wavelength of 633 nm. For anisotropy measurement we used a Perkin-Elmer LS-55 luminescence spectrometer equipped with a filter polarizer

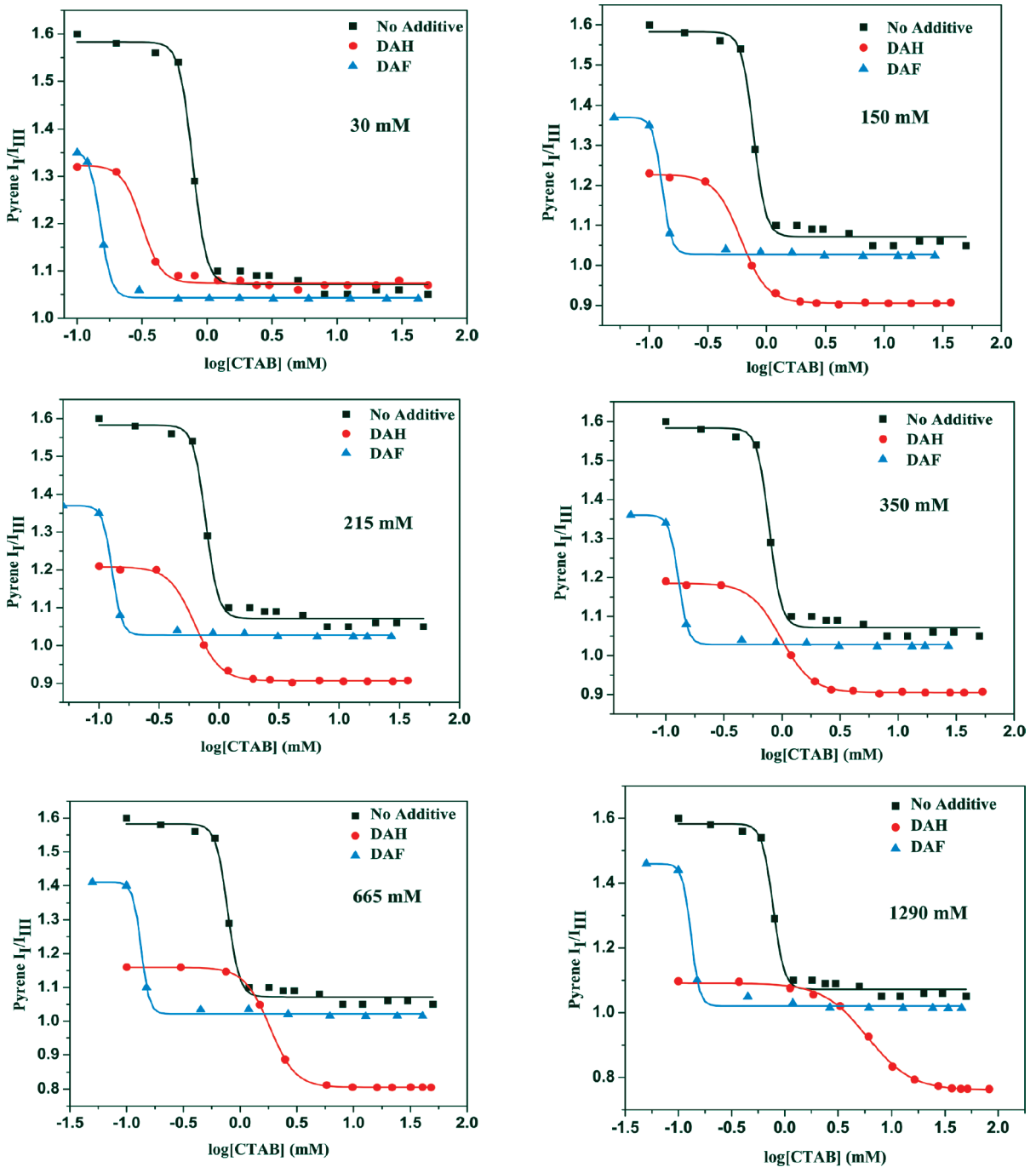

Figure 1. Pyrene (5×10^{-7} M) I_I/I_{III} versus log[CTAB] in the presence of different amounts of DAF and DAH.

and a thermostatted cell holder. Temperature was controlled using a circulating bath (Thermo Neslab, RTE 7).

3. RESULTS

3.1. Determination of CMC from Pyrene Fluorescence. Pyrene has been used to determine CMC due to its unique response to solvent polarity. The change in fluorescence spectrum of pyrene in solvents of different polarities shows that the polarity of an environment can be estimated by measuring the ratio of fluorescence intensities of the first and third vibronic bands, I_I/I_{III} where I_I corresponds to the S_1 ($\nu = 0$) to S_0 ($\nu = 0$) transition, and I_{III} corresponds to the S_1 ($\nu = 0$) to S_0 ($\nu = 1$) transition in pyrene. The I_I/I_{III} decreases with decreasing solvent dipolarity. Figure 1 represents pyrene I_I/I_{III} versus log[CTAB] in the presence of different amounts of both PILs (DAF and DAH). The data were fitted with sigmoidal expression. The CMC values of aqueous CTAB in the presence of different amounts of both PILs (DAF and DAH) are reported in Table 1. The CMC of CTAB decreases from 1.05 mM to 0.52 mM with the addition of 30 mM DAH, but further increase in concentration of DAH up to 1290 mM causes regular increase of CMC up to 20.40 mM. Interestingly, in the case of DAF, only decrease in CMC occurs up to a 1290 mM concentration of DAF. The CMC of CTAB decreases from 1.05 mM to 0.16 mM with the

dx.doi.org/10.1021/jp200233q |J. Phys. Chem. B 2011, 115, 3828–3837

Table 1. CMC Values of Aqueous CTAB in the Presence of Different Amounts of DAF and DAH

	CMC* (mM) from pyrene fluorescence	
concentration of additive (mM)	DAH added	DAF added
0	1.05	1.05
30	0.52	0.20
150	1.06	0.18
215	1.20	0.17
350	1.85	0.17
665	3.70	0.16
1290	20.40	0.16

*±5%.

addition of 1290 mM DAF. So the different role of the two PILs, DAF and DAH, is clearly demonstrated by the variation of CMC of CTAB with the addition of ionic liquids.

3.2. Determination of Micellar Aggregation Number from Fluorescence Quenching Method. The aggregation numbers (N_{agg}) of aqueous CTAB micelle in the presence of different amounts of the PILs DAF and DAH were obtained by observing the fluorescence quenching behavior of pyrene by CPC. The following equation is used for the determination of micellar aggregation number:[51]

$$\ln\left(\frac{I_o}{I_Q}\right) = \langle n\rangle = \frac{Q_{micelle}}{[micelle]} = \frac{[CPC]_{micelle}}{[micelle]} = [CPC]_{micelle}\left[\frac{N_{agg}}{[CTAB] - cmc}\right] \quad (1)$$

where I_o and I_Q are fluorescence intensities of pyrene in the absence and presence of quencher CPC, respectively, $\langle n\rangle$ is the mean occupancy number of the quencher molecule (CPC), $Q_{micelle}$ (i.e., $[CPC]_{micelle}$), [micelle], and [CTAB] are the concentrations of quencher CPC within the micellar phase, micelles, and CTAB surfactant, respectively. Aggregation number is determined from the slope of the $\ln(I_o/I_Q)$ versus $[CPC]_{micelle}$ plot for all the systems. Plots of $\ln(I_o/I_Q)$ versus $[CPC]_{micelle}$ for pyrene quenching by CPC within 150 mM aqueous CTAB in the presence of different amounts of DAF and DAH are shown in Figure 2. The aggregation numbers of aqueous CTAB micelles in the presence of different amounts of both PILs (DAF and DAH) are reported in Table 1. Our result for aqueous CTAB N_{agg} is in good agreement with that reported in the literature. The aggregation number of CTAB increases from 72 to 101 with the addition of 30 mM DAH, but further increase in concentration of DAH up to 1290 mM causes a decrease of aggregation number to 37. Interestingly, in the case of DAF, only increase in aggregation number occurs up to 1290 mM of DAF. The aggregation number of CTAB increases from 72 to 107 with the addition of 1290 mM DAF. So the different role of the two PILs DAF and DAH is re-emphasized by the variation of aggregation number of CTAB with the addition of ILs.

3.3. Determination of Average Aggregate Size from Dynamic Light Scattering. We have used dynamic light scattering (DLS) to obtain the average size of the aggregates of the aqueous CTAB in the presence of different amounts of the PILs DAF and DAH. Figure 3 represents the variation of scattering intensity with the diameter of micellar aggregates. The size of the micellar aggregates in the presence of different amounts of PILs DAF and DAH are reported in Table 2. The size of the aggregate increases from 0.9 to 25.0 nm with the addition of 215 mM DAH, but further increase in concentration of DAH up to 1290 mM causes decrease of aggregate size to 6.7 nm (Figure 4). Once again, in the case of DAF, only increase in aggregate size occurs up to 1290 mM of DAF. The aggregate size increases from 0.9 to 10.2 nm with the addition of 1290 mM DAF. So once again the different role of the two PILs DAF and DAH is emphasized by the variation of aggregate size with the addition of ILs.

3.4. Determination of ζ Potential. We used a Malvern Nano ZS instrument to determine ζ potential of aqueous CTAB in the presence of different amounts of PILs DAF and DAH. Figure 5 represents the variation of ζ potential with the concentration of PILs DAF and DAH. The absolute value of ζ potential decreases as the PILs DAF and DAH are added. ζ potential decreases quite rapidly with the addition of DAH, and it reaches negative value at high concentration of DAH. The ζ potentials of aqueous CTAB in the presence of different amounts of PILs DAF and DAH are reported in Table 3.

3.5. Determination of Conductivity. We have measured electrical conductivity of 150 mM aqueous solutions of CTAB with increasing concentrations of DAF and DAH. Since the solutions are fairly complex and contain micelles, surfactant monomers, and the constituents of DAF and DAH (i.e., dimethylethanol ammonium cation, formate/hexanoate anions, and undissociated IL, if any), it is useless to do any classical treatment based on molar conductivity and electrolyte concentration. Figure 6 represents the variation of conductivity with the concentration of PILs DAF and DAH. The conductivity of aqueous solutions of CTAB increases as the PILs DAF and DAH are added. The conductivities of aqueous CTAB in the presence of different amounts of PILs DAF and DAH are reported in Table 3.

3.6. Determination of Dipolarity of Micellar Pseudophase from Fluorescence Probe Behavior of Pyrene. We have used pyrene I_I/I_{III} to determine the changes in the dipolarity of the micellar pseudophase within 150 mM aqueous solutions of CTAB in the presence of different amounts of DAF and DAH. Figure 7 represents pyrene I_I/I_{III} versus [IL]. The pyrene I_I/I_{III} ratio continuously increases with increasing amount of DAH, whereas in the case of DAF, the pyrene I_I/I_{III} ratio first increases and then almost remains constant.

3.7. Determination of Microfluidity from R6G Fluorescence. The fluorescence anisotropy, which implies the extent of the polarization of the emitted radiation from a probe, depends on the overall geometry of the rotating fluorescence unit as well as the microfluidity of its cybotactic region.[52] Generally, the lower the microfluidity of the immediate environment for a given rotor, the higher the resulting anisotropy. Accordingly, fluorescence anisotropy is a powerful tool to investigate the cybotactic region microfluidity surrounding fluorescent solutes in a variety of complex media such as micelles, microemulsions, polymers, and sol−gel-derived glasses.[52] The steady-state fluorescence anisotropy (r) is given by[52]

$$r = \frac{I_{\parallel} - I_{\perp}}{I_{\parallel} + 2I_{\perp}} \quad (2)$$

where $I_{\parallel}$ and $I_{\perp}$ are the parallelly and perpendicularly polarized components of the emitted radiation from a fluorophore following photoexcitation with vertically polarized light. We have used the "L-format" configuration to measure r for the probe R6G, which is expressed as[52]

$$r = \frac{I_{VV} - GI_{VH}}{I_{VV} + 2GI_{VH}} \quad (3)$$

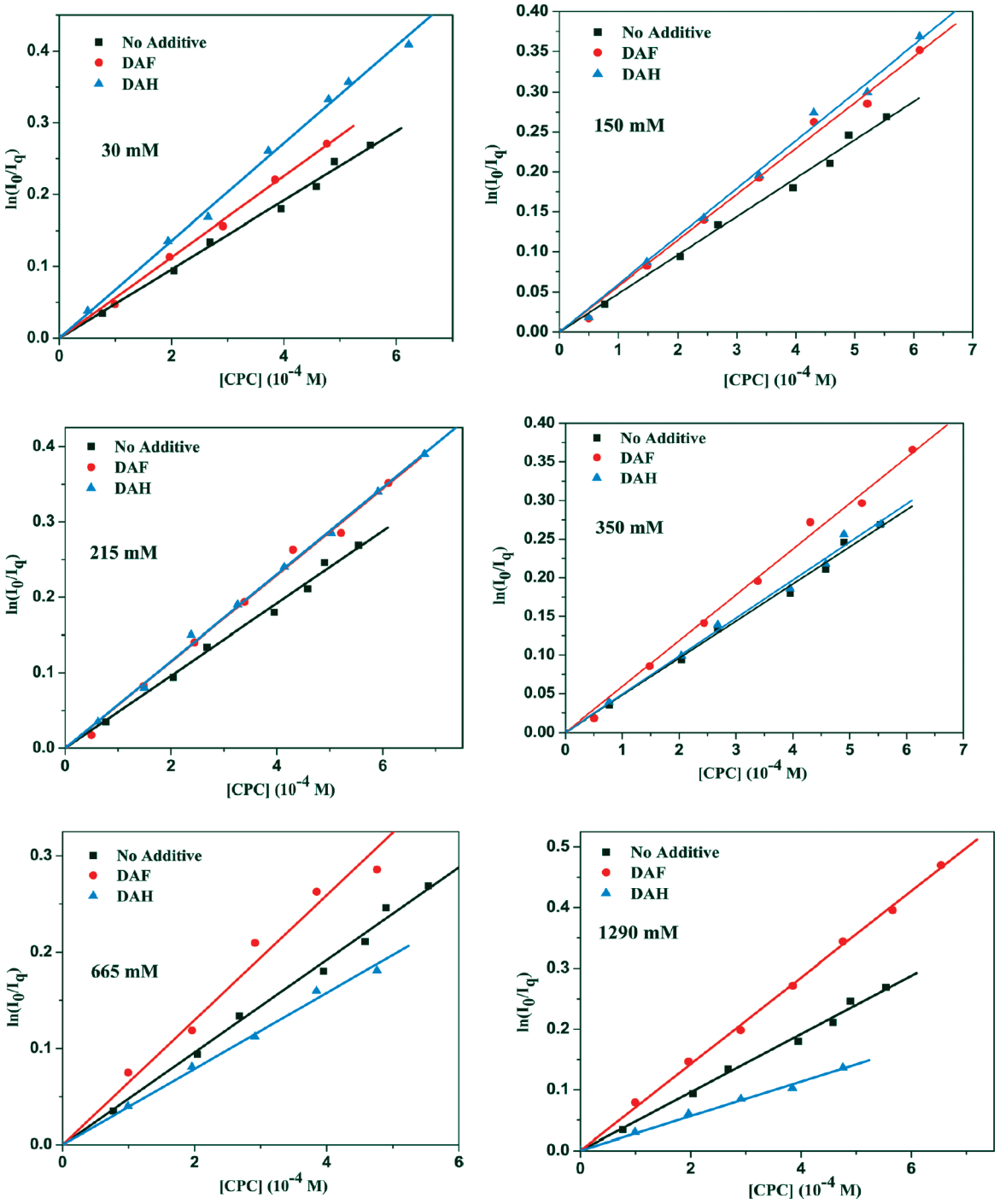

Figure 2. Plots of $\ln(I_o/I_Q)$ versus $[CPC]_{micelle}$ for pyrene (5×10^{-7} M) quenching by CPC within 150 mM aqueous CTAB in the presence of different amounts of DAF and DAH.

$$G = \frac{I_{HV}}{I_{HH}} \tag{4}$$

where I_{VV} and I_{VH} are the vertically and horizontally polarized emission intensities, respectively, resulting from vertically polarized excitation of R6G. While in expression for the G factor I_{HV} and I_{HH} are similarly the vertically and horizontally polarized emissions resulting from horizontally polarized excitation, respectively. Figure 8 represents the variation of steady state anisotropy $\langle r \rangle$ of R6G (1.2 μM) in 150 mM aqueous CTAB with an increasing amount of DAF and DAH. The anisotropy $\langle r \rangle$ of R6G continuously decreases with increasing amount of DAH, whereas a decrease in anisotropy is observed up to 215 mM of DAF addition. With further increase in the concentration of DAF the anisotropy $\langle r \rangle$ of R6G increases.

4. DISCUSSION

Our results clearly demonstrate that the two PILs DAF and DAH modify the properties of aqueous CTAB solution in different way. At lower concentration (i.e., $\leq$ 30 mM) both the ILs show the same

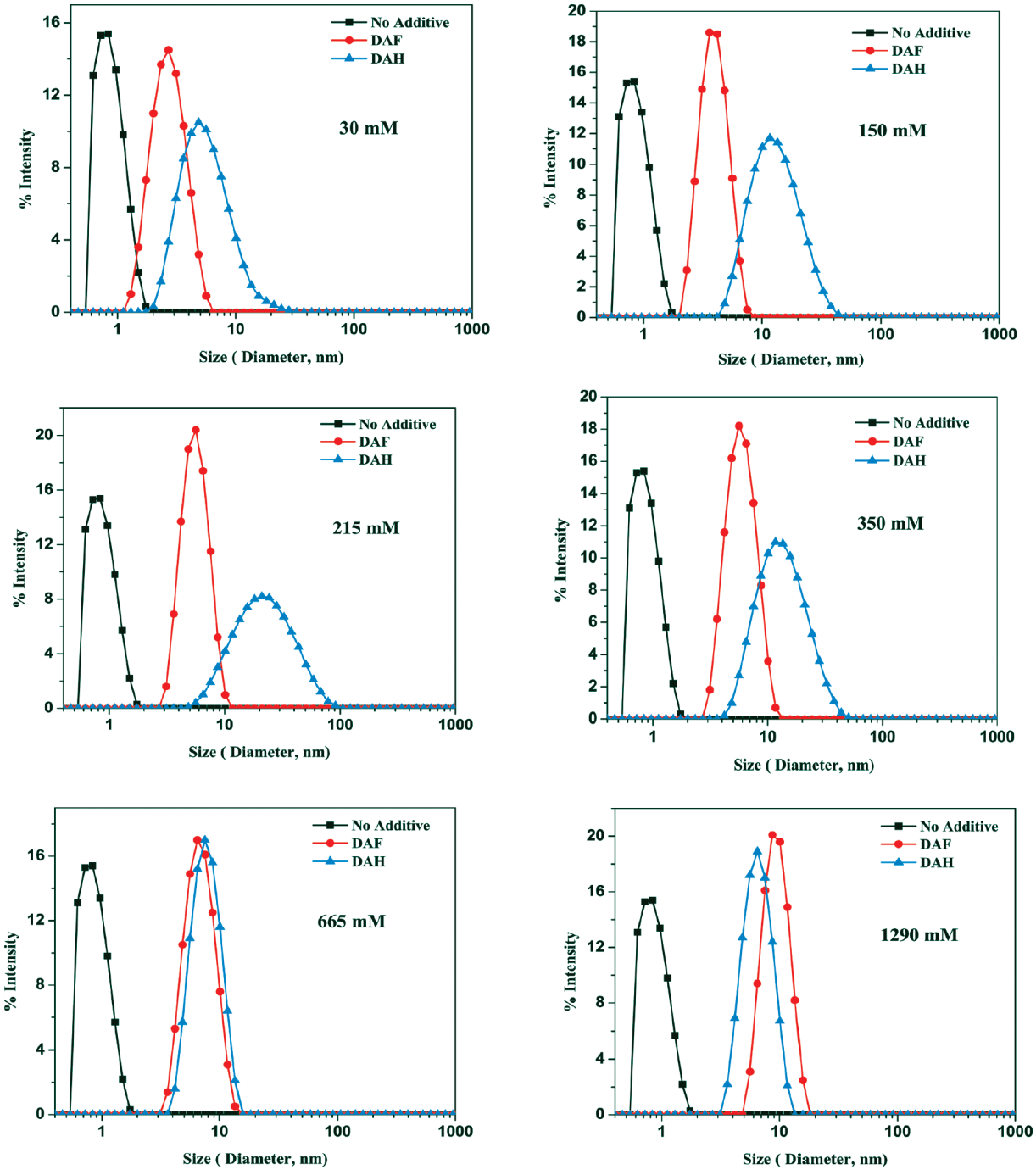

Figure 3. DLS result of 150 mM aqueous CTAB in the presence of different amounts of DAF and DAH.

trend in modifying the properties of aqueous CTAB solution, but DAH as the additive shows a more dramatic increase in aggregation number and size of the CTAB micelle compared to that of DAF as the additive. At higher concentration of additives (DAF and DAH), the properties of aqueous CTAB solution changes in an entirely different way. To account for these differences in the properties of the two PILs, we have to consider the structural differences between the two PILs. Due to its long alkyl chain length, DAH can act as a cosurfactant (penetrating additive), whereas DAF cannot act as a cosurfactant due to the absence of long alkyl chain length (nonpenetrating additive).

The observed trend in CMC, aggregation number, and size with the addition of DAF to the aqueous cationic CTAB solution is the same as that observed for the aqueous CTAB upon addition of KBr[53a] and aqueous HeTAB upon addition of NaBr,[53b] respectively. This clearly indicates the electrolytic behavior of DAF. The observed trend can be explained by the fact that the formate anion of DAF IL undergoes Coulombic attractive interaction with the cationic head groups of CTAB at all concentrations and reduces the repulsive interaction within the positively charged head groups of CTAB. The reduction in repulsive interaction causes stabilization of the micelle and hence

Table 2. Aggregation Number (N_{agg}) and Average Aggregate Size (Diameter) of 150 mM Aqueous CTAB in the Presence of Different Amounts of DAF and DAH

	aggregation number (N_{agg})		size* (diameter, nm)	
concentration of additive (mM)	DAH added	DAF added	DAH added	DAF added
0	72 ± 6	72 ± 6	0.9	0.9
30	101 ± 9	81 ± 9	5.3	2.8
150	90 ± 5	84 ± 6	14.1	4.1
215	83 ± 4	86 ± 5	25.0	5.6
350	74 ± 4	90 ± 5	14.7	6.0
665	58 ± 6	97 ± 4	7.9	7.0
1290	37 ± 6	107 ± 6	6.7	10.2

* ±5%.

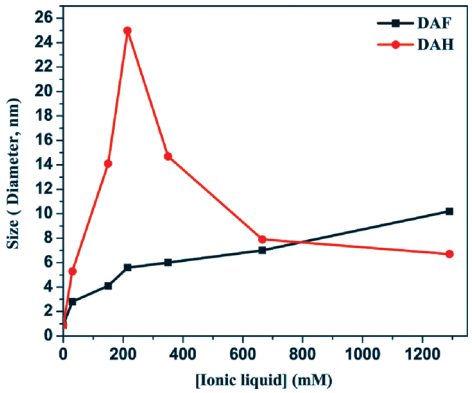

Figure 4. Size (diameter, nm) of 150 mM aqueous CTAB in the presence of different amounts of DAF and DAH.

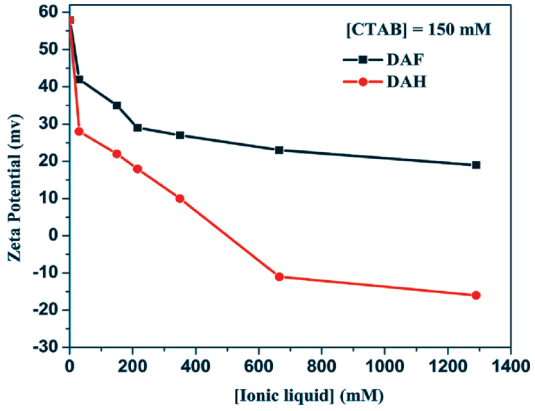

Figure 5. ζ potential of 150 mM aqueous CTAB in the presence of different amounts of DAF and DAH.

the CMC decreases, aggregation number increases, and the size of the micellar aggregate also increases. So we can say that, instead of showing the concentration-dependent dual behavior of ILs,[27a] DAF shows only salt (electrolyte) effect.

The trend in CMC of aqueous CTAB solution on addition of DAH is the same as that observed for the CMC of aqueous cationic CTAB upon addition of [hmim][Br],[54a] aqueous anionic SDS,[27a] and aqueous zwitterionic SB-12[54b] upon addition of [bmim][BF_4] (a decrease at lower [IL] is followed by an increase as the [IL] is increased). So we can conclude that, at lower concentration, DAH also acts as an electrolyte. However, the dramatic increase in size and aggregation number at lower concentration compared to that of DAF indicates the penetration of CTAB micelle by hexanoate anion of the IL. So we can say that the formation of a mixed micelle takes place at lower concentration of DAH due to the presence of the long alkyl chain in the hexanoate anion. It is noteworthy to mention that the decrease in CMC of aqueous CTAB is also observed in the presence of long-chain alcohols possessing cosurfactant-type behavior.[54c] Cosurfactants, such as cationic benzylhexadecyldimethylammonium chloride and nonionic Brij-58, when added at lower concentration, make the CMC of aqueous CTAB lower as well.[54d] The increase in CMC at higher concentrations can be attributed to the fact that DAH can also act as cosolvent at higher concentration, and low solvophobicity between the IL and hydrophobic tail of surfactant molecule leads to a high CMC. This reversal of the role of the IL (DAH) at higher concentration is well supported by earlier reports.[27a,54a,54b]

In the same way, the decreases in aggregation number N_{agg} at higher concentration of DAH confirms the cosolvent nature of DAH at higher concentration. Cosolvents such as glycerol, ethylene glycol, and phenol present at higher concentrations within aqueous CTAB also result in decreased N_{agg}. Additionally, Behera et al. have reported that addition of [bmim][BF4] to aqueous nonionic Triton X-100,[27b] anionic SDS,[27a] and zwitterionic SB-12[54b] shows the cosolvent nature of IL and decrease in N_{agg} at higher concentrations of IL ([bmim][BF4]).

The size of the CTAB micelle was found to be 0.9 nm. Interestingly, with the addition of 215 mM DAH, the size of the CTAB micellar aggregate increases to 25.0 nm, whereas with the addition of 215 mM DAF it increases to only 5.6 nm. Addition of *n*-butanol, *n*-pentanol, and *n*-hexanol, respectively, also result in increased average micellar hydrodynamic diameter of aqueous alkanediyl-α,ω-bis(dimethylcetylammonium bromide), a gemini surfactant. Importantly, the extent of increase is more as the alkyl chain length of the alcohol is increased (i.e., increasing the cosurfactant nature of the alcohol).[55] It is proposed that the formate and hexanoate anions undergo Coulombic attractive interaction with cationic head groups of CTAB micelle at all concentrations. In the case of DAH, the presence of a hexyl chain on the hexanoate ion allows it to align with the tail part of CTAB, whereas, in the case of DAF, the absence of an alkyl chain in the formate ion is apparently unable to align the formate anion with the tail part of CTAB. So this difference in the location of the anions of DAF and DAH is responsible for the different size changes and different behaviors of the two ILs. At higher concentration of DAH, the decrease in size of the CTAB micellar aggregate once again confirms the cosolvent nature of DAH

Table 3. Conductivity and ζ Potential of 150 mM Aqueous CTAB in the Presence of Different Amounts of DAF and DAH

	conductivity* (ms/cm)		ζ potential* (mv)	
concentration of additive (mM)	DAH added	DAF added	DAH added	DAF added
0	4.5	4.5	58	58
30	6.1	5.7	28	42
150	10.8	12.0	22	35
215	15.2	17.5	18	29
350	18.2	22.4	10	27
665	26.5	35.1	−11	23
1290	29.5	52.6	−16	19

*±5%.

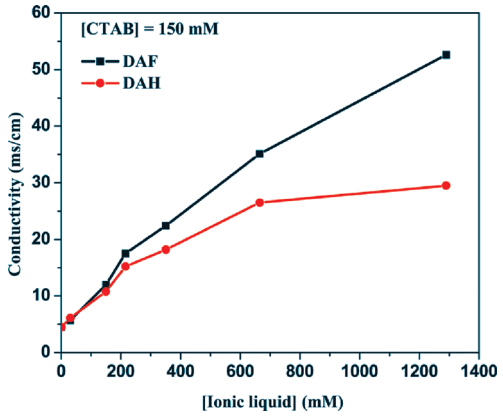

Figure 6. Conductivity of 150 mM aqueous CTAB in the presence of different amounts of DAF and DAH.

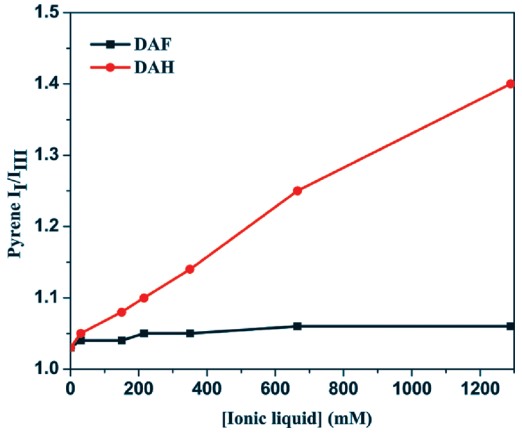

Figure 7. Pyrene (5×10^{-7} M) I_I/I_{III} in 150 mM aqueous CTAB in the presence of different amounts of DAF and DAH.

at higher concentrations. The decrease in size of the CTAB micellar aggregate at higher concentrations of DAH is also supported by the decrease in size at higher concentrations of IL [bmim][BF4] when added to aqueous anionic SDS.[27a]

The absolute value of ζ potential is the potential difference between the dispersion medium and the stationary layer of fluid attached to the dispersed micellar aggregates. The ζ potential indicates the degree of repulsion between adjacent similarly charged aggregates in the solution. The magnitude of the ζ potential gives an indication of the potential stability of the colloidal system. A decrease in ζ potential clearly hints at diminishing surface charge of our cationic micellar aggregates that is a consequence of the interaction of cationic surface with formate and hexanoate anion of the ILs. The rapid decrease of ζ potential with the addition of DAH, following negative values at higher concentrations, clearly indicates very strong interaction of DAH with a cationic surface of CTAB micellar aggregate. This can be attributed to the presence of a long alkyl chain in the hexanoate ion, which helps in the incorporation of DAH in the micellar system.

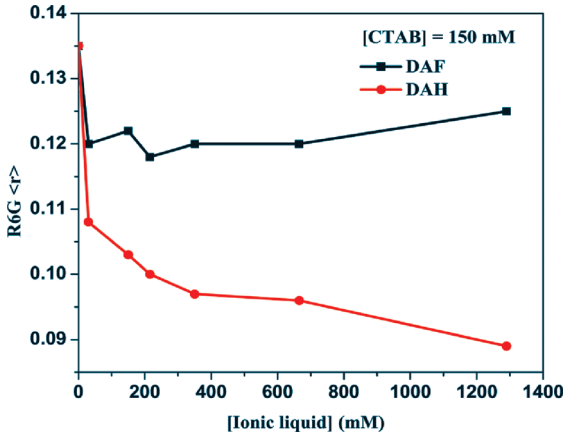

Figure 8. Steady state anisotropy ⟨r⟩ of R6G (1.2 μM) in 150 mM aqueous CTAB in the presence of different amounts of DAF and DAH.

The absolute value of conductivity of DAF-added CTAB solution is always higher than that of DAH-added CTAB solution. The conductivity increases almost linearly with the addition of DAF, whereas in case of DAH, the variation is not linear in nature. This also indicates very strong interaction of DAH with cationic surface of CTAB micelle. This can be once again attributed to the presence of a long alkyl chain in the hexanoate ion, which helps in the incorporation of DAH in the micellar system.

Figure 7, which represents pyrene I_I/I_{III} for postmicellar aqueous CTAB in the presence of DAF and DAH, respectively, clearly indicates that pyrene I_I/I_{III} appears to be independent of the presence of DAF. This indicates that the cybotactic region of pyrene remains unchanged by the addition of DAF. In the case of DAH addition, the pyrene I_I/I_{III} increases almost linearly. It is well established that, on average, pyrene locates itself in the palisade layer of the micellar pseudophase,[56] so increase in pyrene I_I/I_{III} clearly indicates that the cybotactic region is modified by the addition of DAH, which further confirms the penetration of the CTAB micelle by DAH.

dx.doi.org/10.1021/jp200233q |J. Phys. Chem. B 2011, 115, 3828–3837

The most counterintuitive result is the variation of the microfluidity of R6G with the addition of DAF and DAH, respectively. Due to relatively high viscosity of ILs it is quite expected that the addition of IL to aqueous CTAB solution will reduce the microfluidity, but we have observed the reverse. At lower concentration of PILs DAF and DAH, the anisotropy value changes rapidly, but once again it changes more rapidly in the case of DAH. This increase in microfluidity with the addition of IL can be attributed to an increase in water penetration to the micellar phase. This water penetration is also supported by the huge increase in size at lower concentrations of PILs. Apparently, the anisotropy value clearly suggests more water penetration in the case of DAH. Once again it can be attributed to the presence of a long alkyl chain in the hexanoate ion, which helps in the incorporation of DAH in the micellar system and hence increases water penetration.

5. CONCLUSION

In conclusion, we can say that PIL can also be used to modify the properties of conventional micelles in a controlled fashion. Here, formate and hexanoate anions of DAF and DAH, respectively, act as oppositely charged counterions for cationic CTAB micelle and hence favor the micellization process. Nevertheless, a clear change is observed in the physicochemical behavior of aqueous solutions of CTAB at higher concentrations of DAF and DAH. The alkyl chain present on the anion of DAH leads to its partitioning into the CTAB−DAH interface and behaves as a cosurfactant, whereas DAF having no alkyl chain on the formate anion shows an almost pure salt effect. This type of mixed micelle (DAH-incorporated CTAB micelle), where the PILs act as cosurfactants, may have enormous future application for conducting interfacial reactions and micellar catalysis. Additionally, since the micelle exists with the addition of 1290 mM and even more (in the case of DAF, the micelle exist even at 3 M concentration) PILs, in the future, this type of system might be used in proton exchange fuel cells at temperatures in excess of 100 °C.

AUTHOR INFORMATION

Corresponding Author

*E-mail: nilmoni@chem.iitkgp.ernet.in. Fax: 91-3222-255303.

ACKNOWLEDGMENT

N.S. is thankful to the Department of Science and Technology (DST), and Board of Research in Nuclear Sciences (BRNS), Government of India, for generous research grants. V.G.R, C.G., R.P., and S.M. are thankful to CSIR for a research fellowship. S.S. is thankful to BRNS for an SRF.

REFERENCES

(1) Jaramillo, T. F.; Baeck, S. H.; Cuenya, B. R.; McFarland, E. W. *J. Am. Chem. Soc.* **2003**, *125*, 7148.

(2) Sohn, B. H.; Choi, J. M.; Yoo, S. I.; Yun, S. H.; Zin, W. C.; Jung, J. C.; Kanehara, M.; Hirata, T.; Teranishi, T. *J. Am. Chem. Soc.* **2003**, *125*, 6368.

(3) Massey, J. A.; Winnik, M. A.; Manners, I.; Chan, V. Z. H.; Ostermann, J. M.; Enchelmaier, R.; Spatz, J. P.; Moller, M. *J. Am. Chem. Soc.* **2001**, *123*, 3147.

(4) Savic, R.; Luo, L. B.; Eisenberg, A.; Maysinger, D. *Science* **2003**, *300*, 615.

(5) Allen, C.; Maysinger, D.; Eisenberg, A. *Colloids Surf., B* **1999**, *16*, 3.

(6) Alexandridis, P., Lindman, B., Eds.; *Amphiphilic Block Copolymers: Self-Assembly and Applications*; Elsevier: Amsterdam, 2000.

(7) He, Y. Y.; Li, Z. B.; Simone, P.; Lodge, T. P. *J. Am. Chem. Soc.* **2001**, *128*, 2745.

(8) Palepu, R. M.; Gharibi, H.; Bloor, D. M.; Wyn-Jones, E. *Langmuir* **1993**, *9*, 110.

(9) Lee, Y. S.; Woo, K. W. *J. Colloid Interface Sci.* **1995**, *169*, 34.

(10) Evans, D. F. *Langmuir* **1988**, *4*, 3.

(11) Ward, A. J. I.; du Reau, C. Surfactant Association in Nonaqueous Media. In *Surface and Colloid Science*; Matijevic, E., Ed.; Plenum Press: New York, 1993; Vol. 15, Chapter 4.

(12) Anderson, J. L.; Pino, V.; Hagberg, E. C.; Sheares, V. V.; Armstrong, D. W. *Chem. Commun.* **2003**, *19*, 2444.

(13) Evans, D. F.; Yamauchi, A.; Wei, G. J.; Bloomfield, V. A. *J. Phys. Chem.* **1983**, *87*, 3537.

(14) Atkin, R.; Warr, G. G. *J. Am. Chem. Soc.* **2005**, *127*, 11940.

(15) Eastoe, J.; Gold, S.; Rogers, S. E.; Paul, A.; Welton, T.; Heenan, R. K. *J. Am. Chem. Soc.* **2005**, *127*, 7302.

(16) Gao, H. X.; Li, J. C.; Han, B. X.; Chen, W. N.; Zhang, J. L.; Zhang, R. *Phys. Chem. Chem. Phys.* **2004**, *6*, 2914.

(17) Gao, Y. A.; Li, N.; Zheng, L. Q.; Zhao, X. Y.; Zhang, S. H.; Han, B. X. *Green Chem.* **2006**, *8*, 43.

(18) Greaves, T. L.; Weerawardena, A.; Fong, C.; Drummond, C. J. *Langmuir* **2007**, *23*, 402.

(19) Lee, J.; Panzer, M. J.; He, Y.; Lodge, T. P.; Frisbie, C. D. *J. Am. Chem. Soc.* **2007**, *129*, 4532.

(20) Hao, J. C.; Song, A. X.; Wang, J. Z.; Chen, X.; Zhuang, W. C.; Shi, F. *Chem.—Eur. J.* **2005**, *11*, 3936.

(21) Emerson, M. F.; Holtzer, A. *J. Phys. Chem.* **1967**, *71*, 3320.

(22) Shirahama, K.; Kashiwabara, T. *J. Colloid Interface Sci.* **1971**, *36*, 65.

(23) Ward, A. F. *Proc. R. Soc. A* **1940**, *176*, 412.

(24) Malik, W. U.; Verma, S. P.; Crand, P. *Indian J. Chem.* **1970**, *8*, 826.

(25) Frank, H. S. *Fed. Proc., Suppl.* **1965**, *15*, 51.

(26) Scheraga, H. A. *Ann. N.Y. Acad. Sci.* **1965**, *125*, 253.

(27) (a) Behera, K.; Pandey, S. *J. Phys. Chem. B* **2007**, *111*, 13307. (b) Behera, K.; Pandey, M. D.; Porel, M.; Pandey, S. *J. Chem. Phys.* **2007**, *127*, 184501.

(28) Shimizu, S; McLaren, W. M.; Matubayasi, N. *J. Chem. Phys.* **2006**, *124*, 234905.

(29) Zheng, L.; Guo, C.; Wang, J.; Liang, X.; Chen, S.; Ma, J.; Yang, B.; Jiang, Y.; Liu, H. *J. Phys. Chem. B* **2007**, *111*, 1327.

(30) Dey, S.; Adhikari, A.; Das, D. K.; Sasmal, D. K.; Bhattacharyya, K. *J. Phys. Chem. B* **2009**, *113*, 959.

(31) Greaves, T. L.; Drummond, C. J. *Chem. Rev.* **2008**, *108*, 206.

(32) Evans, D. F. *Langmuir* **1988**, *4*, 3.

(33) Araos, M. U.; Warr, G. G. *J. Phys. Chem. B* **2005**, *109*, 14275.

(34) Spicer, P. T.; Small, W. B.; Lynch, M. L. Patent WO066014-A2, 2002.

(35) Greaves, T. L.; Weerawardena, A.; Fong, C.; Drummond, C. J. *J. Phys. Chem. B* **2007**, *111*, 4082.

(36) Zhao, G. Y.; Jiang, T.; Gao, H. X.; Han, B. X.; Huang, J.; Sun, D. H. *Green Chem.* **2004**, *6*, 75.

(37) Janus, E.; Goc-Maciejewska, I.; Lozynski, M.; Pernak, J. *Tetrahedron Lett.* **2006**, *47*, 4079.

(38) Lansalot-Matras, C.; Moreau, C. *Catal. Commun.* **2003**, *4* 517.

(39) Garlitz, J. A.; Summers, C. A.; Flowers, R. A.; Borgstahl, G. E. O. *Acta Crystallogr., Sect. D* **1999**, *55*, 2037.

(40) Lau, R. M.; Sorgedrager, M. J.; Carrea, G.; Van Rantwijk, F.; Secundo, F.; Sheldon, R. A. *Green Chem.* **2004**, *6*, 483.

(41) Angell, C. A.; Wang, L. M. *Biophys. Chem.* **2003**, *105*, 621.

(42) Pernak, J.; Goc, I.; Fojutowski, A. *Holzforschung* **2005**, *59*, 473.

(43) Noda, A.; Susan, M. A. B. H.; Kudo, K.; Mitsushima, S.; Hayamizu, K.; Watanabe, M. *J. Phys. Chem. B* **2003**, *107*, 4024.

(44) Sun, J. Z.; Jordan, L. R.; Forsyth, M.; Macfarlane, D. R. *Electrochim. Acta* **2001**, *46*, 1703.
(45) Angell, C. A.; Xu, W.; Belieres, J.-P.; Yoshizawa, M. Patent WO114445, 2004.
(46) Galvez-Ruiz, J. C.; Holl, G.; Karaghiosoff, K.; Klapotke, T. M.; Loehnwitz, K.; Mayer, P.; Noeth, H.; Polborn, K.; Rohbogner, C. J.; Suter, M.; Weigand, J. J. *Inorg. Chem.* **2005**, *44*, 4237.
(47) Drake, G. W.; Hawkins, T. W.; Boatz, J.; Hall, L.; Vij, A. *Propellants, Explos., Pyrotech.* **2005**, *30*, 156.
(48) Gutowski, K. E.; Holbrey, J. D.; Rogers, R. D.; Dixon, D. A. *J. Phys. Chem. B* **2005**, *109*, 23196.
(49) Huang, J. F.; Luo, H.; Liang, C.; Sun, I. W.; Baker, G. A.; Dai, S. *J. Am. Chem. Soc.* **2005**, *127*, 12784.
(50) Xu, W.; Angell, C. A. *Science* **2003**, *302*, 422.
(51) (a) Turro, N. J.; Yekta, A. *J. Am. Chem. Soc.* **1978**, *100*, 5951. (b) Sabate, R.; Estelrich, J. *J. Phys. Chem. B* **2003**, *107*, 4137. (c) Tachiya, M. *Chem. Phys. Lett.* **1975**, *33*, 289. (d) Tachiya, M. *J. Chem. Phys.* **1982**, *76*, 340. (d) Karukstis, K. K.; McDonough, J. R. *Langmuir* **2005**, *21*, 5716.
(52) Lakowicz, J. R. *Principles of Fluorescence Spectroscopy*, 3rd ed.; Kluwer Academics/Plenum Publishers: New York, 2006.
(53) (a) Singh, H. N.; Swarup, S.; Salim, S. M. *J. Colloid Interface Sci.* **1979**, *68*, 128. (b) Mosquera, V.; Rıo, J. M.; Attwood, D.; Garcia, M.; Jones, M. N.; Prieto, G.; Suarez, M. J.; Sarmiento, F. *J. Colloid Interface Sci.* **1998**, *206*, 66.
(54) (a) Behera, K.; Om, H.; Pandey, S. *J. Phys. Chem. B* **2009**, *113*, 786. (b) Behera, K.; Pandey, S. *Langmuir* **2008**, *24*, 6462. (c) Munoz, M.; Graciani, M. D. M.; Rodriguez, A.; Moya, M. L. *Int. J. Chem. Kinet.* **2004**, *36*, 634. (d) Dar, A. A.; Rather, G. M.; Das, A. R. *J. Phys. Chem. B* **2007**, *111*, 3122.
(55) Siddiqui, U. S.; Ghosh, G.; Din, K. *Langmuir* **2006**, *22*, 9874.
(56) (a) Thomas, J. K. *Chem. Rev.* **1980**, *80*, 283. (b) Almgren, M.; Grieser, F.; Thomas, J. K. *J. Am. Chem. Soc.* **1979**, *101*, 279. (c) Lianos, P.; Viriot, M. L.; Zana, R. *J. Phys. Chem.* **1984**, *88*, 1098.